Breast Cancer Research

RESEARCH

Open Access

Multi-receptor targeted therapy of breast cancer and brain metastases with a novel QUAD-drug conjugate

Waldemar Debinski[1,6*], Kaitlin N. Fink[1], John Rossmeisl[2], Ryan T. Mott[3], Kounosuke Watabe[1], Ralph D'Agostino[4], Alexandra Thomas[5] and Denise Herpai[1]

Abstract

Background Identifying treatments for triple-negative breast cancer (TNBC) remains a critical medical need. We have found that Interleukin 13 receptor alpha 2 (IL-13RA2), EphA2, EphA3 and EphB2 receptors are over-expressed collectively in majority of patients with breast cancer and its brain metastases. We are pursuing the novel idea of targeting these four tumor-associated receptors identified by us with one pharmaceutical compound. A compound, called QUAD, was designed and constructed, which binds all four targeted receptors.

Methods We have examined the presence of IL-13RA2, EphA2, EphA3 and EphB2 receptors in breast cancer cells in vitro, tissue micro-arrays including involved lymph nodes, and in paired primary tumor—brain metastases, including two subtypes of breast cancer. We also tested the activity of the quadrivalent ligand, QUAD, conjugated to a derivative of maytansine, DM1, in vitro and in vivo.

Results We have found that the four target receptors are frequently over-expressed in breast cancer, including TNBC and (HER2)-positive breast cancers and related metastases to the brain. This is based on the observed expression levels for the genes and the gene products; a combined expression of our target of interest approaches 100% of specimens' positivity. Furthermore, several TNBC cell lines were killed at low concentrations of QUAD-DM1 conjugate. MDA-MB-231 tumors growing in mammary pads of athymic mice responded significantly to a dose of 12 mg/kg (3x). MDA-MB-231-BrM tumors growing intracranially also responded to 4 µg/mouse (1x) of QUAD-DM1.

Conclusions QUAD-DM1 is a novel multivalent drug conjugate that appears to be highly suitable for the treatment of breast cancer and related brain metastases. The drug candidate can be administered systemically, due to its favorable toxicity profile, or loco-regionally.

Keywords Breast cancer, Breast cancer brain metastases, Triple-negative breast cancer (TNBC), Interleukin 13 receptor alpha 2 (IL-13RA2), EphA3, EphA2 and EphB2 receptors, Mammary fat pad tumor, Intracranial tumor, QUAD, A ligand binding four receptors, DM1, Maytansine

*Correspondence:
Waldemar Debinski
debinski@wakehealth.edu
Full list of author information is available at the end of the article

Background

More than 300,000 new cases of invasive breast cancer are diagnosed in the US yearly. Triple negative breast cancer (TNBC), which lacks expression of estrogen (ER), progesterone (PR) and epidermal growth factor 2 (HER2) receptors, represent ~ 15% of breast cancers (~ 45,000 patients/year) [1–3]. TNBC displays an aggressive clinical phenotype, with ~ 25% relapsing with metastatic disease. TNBC disproportionately affects black, latinx and women (< 50 years old) [4, 5]. Brain metastases from breast cancer (BMBC) constitute the second most common cause of brain metastasis and TNBC is frequently associated with brain metastases. Thus, BMBC and especially TNBC and its brain metastases are unmet needs in medicine. Major progress in molecular biology and drug development have enabled HER2-positive breast cancer to become manageable [6, 7].

In our current work, we present data obtained from research that was initially intended to exploit breast cancer as putatively negative or a low expressor for the set of four specific target receptors: IL-13RA2, EphA2, EphA3, and EphB2. We previously discovered these receptors in most glioblastoma (GBM) patients, but not in normal brain. IL-13RA2 is a monomeric receptor to which only IL-13 binds, unlike its normal tissue counterpart, IL-13RA1/IL-4A, which binds both IL-13 and IL-4 [8]. Also, IL-13RA1/IL-4A is expressed on T cells among many other normal cells and thus is not a favored target for therapies [9]. In addition, IL-13RA2 mediates IL-13 signaling in cancer cells [10]. We also discovered significant over-expression of an EphA2 receptor in GBM [11–14]. EphA2 belongs to the largest protein tyrosine kinase receptor family in eukaryotes [15–17]; these receptors are bound by natural ligands called ephrins. EphA2 is over-expressed in up to 60% of patients with GBM [12, 18], while ~ 90% of all GBM over-express IL-13RA2 and/or EphA2 that are absent in normal brain [11]. Expression of gene/protein correlates with glioma patients' survival [18–20]. IL-13RA2 and EphA2 are expressed in locally infiltrating GBM cells, and EphA2 is over-expressed on abnormal endothelium of tumor-associated vessels [11, 21–24]. EphA2 activation by its preferred ligand, ephrin-A1 (eA1), inhibits anchorage-independent growth and invasiveness of GBM cells [13, 22, 23]. EphA2 is also important for the self-renewing and tumorigenic potential of GBM stem-like cells (GSCs) [25, 26]. Thus, IL-13RA2 and EphA2 are attractive therapeutic targets [11, 25, 27]. EphA3 receptor is over-expressed in > 50% of GBM specimens, but not normal brain [28]. It correlates with survival in a mesenchymal group, and it is important for the self-renewing potential and tumorigenicity of GSCs [29]. We also found EphA3 receptors in an M2 subgroup of tumor-associated macrophages (TAMs) [28]. Furthermore, the EphB2 receptor, the fourth targeted by QUAD, has been shown to take part in regulation of glioma cells adhesion, growth and invasion [30]. EphB2 is also important in many other cancer types by exhibiting tumor-promoting and tumor-suppressing activities [31]. Thus, the EphB2 receptor is potentially attractive for therapeutic targeting and/or delivery of drug conjugates. These findings widened the spectrum of tumor compartments that can be exploited in targeted therapies.

Considering the patterns of overexpression for EphA2, EphA3, and EphB2 receptors along with IL-13RA2, combinatorial targeting of these receptors leads to coverage of an entire tumor microenvironment. This follows our previous successful proposal to target IL-13RA2 and EphA2 with a cocktail of targeted cytotoxins [32] or, EphA2, EphA3, and EphB2 receptors with one cytotoxin [33]. It is anticipated that antigen loss could be potentially avoided when simultaneously targeting multiple receptors, which is highly relevant to the treatment of breast cancer.

As planned in control experiments for specificity of brain tumors targeting, we unexpectedly found that EphA2, EphA3, EphB2 and IL-13RA2, receptors are highly present in breast cancer and breast cancer brain metastases. Our results strongly suggest that a drug candidate, QUAD-DM1, targeting all four of these receptors can also be effective in the treatment of breast cancer and its brain metastases. BCBM and TNBC are of poor prognosis, hence QUAD targeting these cancers may offer a new way of managing them.

Methods

QUAD is a multivalent protein ligand binding preferentially to four receptors: EphA2, EphA3, EphB2 and IL-13RA2. The DNA sequence for QUAD is *il-13 M-ch2ch3-ea5* plus additional cysteine residues at the C-terminal ends of the protein chains. The binding to the three Eph receptors is contained in the ephrinA5 (eA5) ligand. IL-13 M was modified for receptor binding optimization. The cysteines serve as specific conjugation sites to anti-cancer drugs/toxins (Fig. 1) like DM1-SMCC.

Cell lines and reagents

MDA-MB-231, ZR-75, T47D and Sk-Br-3 cells were received from the American Type Culture Collection (ATCC). BT549, HCC1806, and MDA-MB-468 were obtained from Dr. Watabe. MDA-MB-231, HCC1806, MDA-MB-468, and BT549 cells are TNBC cells [34]. The remaining breast cancer cells were from laboratory stock. MDA-MB-231 BrM cells (TNBC and brain metastatic) were obtained from Dr. Joan Masague. Paclitaxel [35], which targets tubulin, and Capeticabine [36], which inhibits the synthesis of thymidine monophosphate, were obtained from MedChem Express. All breast and GBM

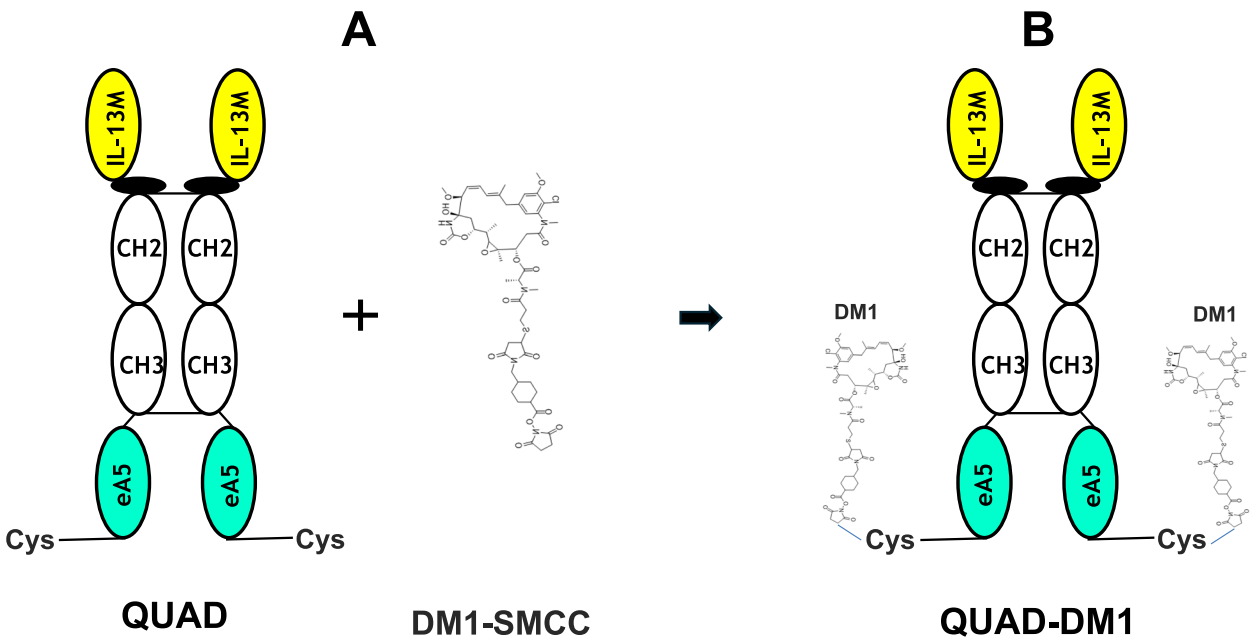

Fig. 1 Schemata of QUAD and its conjugate with DM1. **A** Schematic presentation of QUAD conjugation to DM1 to produce QUAD-DM1. **B** General structure of QUAD-DM1. The DNA sequence for QUAD is *il-13 M-ch2ch3-ea5* plus additional cysteine residues at the C-terminal ends of the protein chains. The cysteines serve as specific conjugation sites to anti-cancer drugs/toxins like DM1-SMCC

cancer cell lines were authenticated by IDEXX Bioanalytics (Columbia, MO) by 16 allele STR.

Purification of QUAD

QUAD was produced in a High Five insect expression system as previously described [33]. Fractions containing the desired protein were pooled, concentrated and buffer exchanged to PBS containing 5 mM EDTA.

QUAD conjugation with DM1-SMCC (derivative of maytansine)

QUAD protein was diluted to 1 µg/µL. DM1-SMCC (AdooQ Biosciences, cat# A15955) was slowly added dropwise while stirring at a 1:16 molar ratio. Mixture continued stirring at room temperature for 1 h. Reaction was allowed to continue stirring overnight at 4 °C. Reaction mixture was centrifuged to remove any precipitation. The resulting QUAD-DM1 conjugate was desalted with Zeba spin columns (Pierce Biotechnology, Rockford, IL cat# A57759) to remove any unconjugated DM1. Successful conjugation was confirmed by a shift on non-reducing SDS-PAGE.

Trastuzumab conjugation with DM1-SMCC

Biosimilar Trastuzumab (Bio X Cell, Lebanon, NH, cat# SIM0005) was treated with SPDP (Pierce, Rockford, IL, cat# 21,857) at a 1:10 molar ratio to generate sulfhydryl groups. TCEP (Gold Biotechnology, St Louis, MO cat# TCEP1) (1:5 molar ratio) was used to generate free thiols. DM1-SMCC was slowly added in a 1:8.3 molar ratio and allowed to stir overnight at 4 °C. The solution was then treated with NEM (Thermo Fisher, Waltham, MA cat # L00355) at a 1:10 molar ratio to cap the reaction.

Western blots

Western blot analysis was conducted as previously described [11]. Primary antibodies included EphA2 (clone D7 purified in house), EphA3 (MyBiosource, San Diego, CA, cat# MBS821916), EphB2 (R&D Systems, Minneapolis, MN, cat# AF467), IL-13RA2 (HUABIO Woburn Massachusetts cat# HA722051), PLK-1 antibody 1:1000 (Genetex, cat# GTX15779 Irvine, CA), and Her2 1:1000 (Cell Signaling, cat# 4290 Danvers, MA). Western blot of QUAD, QUAD-DM1, biosimilar of Trastuzumab and T-DM1 (made in house) were performed with anti-DM1 antibody (HUABIO, Woburn, MA cat# HA600013, 1:2000) and anti-human IgG HRP antibody (Jackson Immuno, West Grove, PA, cat# 709–005-149).

Flow cytometry

Flow cytometry was performed as previously described [32]. Briefly, cells were detached with Versene and washed once with PBS. 200,000 cells in PBS/1% BSA

were aliquoted and incubated on ice for 1 h to block non-specific sites. 2.0 µg of QUAD protein or human Fc control was added to the tubes and incubated on ice for 2 h. After washing with PBS/1% BSA, secondary antibody was added (anti-human Alexa fluor 647, Invitrogen cat # A-21249). Following 1 h incubation on ice, cells were washed and fixed with formalin. Detection was performed on an Accuri6 flow cytometer (BD Biosciences), and data were analyzed with FCS Express (DeNovo Software).

Specificity of QUAD-DM1 killing action in breast cancer cells

200 nM of unconjugated QUAD was added at each concentration of QUAD-DM1. Cells treated with cycloheximide served as a treated control. After 72 h of incubation, cell viability was determined using a colorimetric Thiazolyl Blue Tetrazolium Bromide (MTT) (Gold Biotechnologies cat# T-030) [37]. Absorbance was measured at 570 nm.

Cell cycle analysis

Log phase MDA-MB-231 cells were serum-starved for 24 h. Normal growth media containing 1 nM QUAD-DM1 or unconjugated QUAD or human Fc [made in house (sham)] was applied. Nuclei were stained with Propidium Iodide containing RNAseA (BD Biosciences, Milpitas, California, cat# 550,825). Cell cycle data was collected on a Canto II Flow Cytometer (BD Bioscience). Multicycle DNA analysis was performed with FCS Express (DeNovo Software).

Measurement of PLK-1

1.5×10^5 MDA-MB-231 and 1.5×10^5 MDA-MB-231-BrM cells were plated in a 6 well culture plate and allowed to grow overnight. Both cell lines were treated with 1 nM QUAD-DM1 and for untreated controls cell media was replaced. After 24 h, cell lysates were collected. Proteins were detected via western blot, as stated above with PLK-1 primary antibody (Genetex). β-actin was used for loading control and normalized for analysis of increase in PLK-1 expression with Amersham RGB600 ImageQuant TL Software.

Histone phospho-serine and Aurora A staining

2×10^4 MDA-MB-231 cells were plated on glass coverslips and allowed to adhere overnight at 37 °C with 5% CO2. Media was replaced with serum-free media for 24 h. Cells were treated with 1 nM QUAD-DM1 in serum containing media. Media from control untreated cells was replaced with media containing serum. After 24 h, cells were fixed with formalin followed by permeabilization with PBS/1% BSA/0.1% Triton X-100. Primary antibody was applied and allowed to be incubated for 1 h at room temperature. Antibodies included Aurora A 1:500 (Cell Signaling, cat# 12,100 Danvers, MA) and Histone H3S10ph (phosphor Ser10) 1:500, (Genetex cat# HL1752 Ivine, CA). Coverslips were washed prior to the addition of alexa-fluor conjugated secondary antibodies (Invitrogen Waltham, Massachusetts). Following 1 h incubation, coverslips were washed, inverted onto glass slides and mounted with Fluormount-G containing DAPI) (Southern Biotech, Birmingham, AL). Twenty random fields were photographed per treatment using an Olympus IX70 inverted microscope and CellSens imaging software. Total and stained cells per field were counted. Data is presented as the average percent cells stained per field.

Anti-tumor experiments in vivo

Peripheral tumors

Nude mice were injected into the fourth mammary fat pad with 500,000 MDA-MB-231 cells in a volume of 100 µl. Tumors were measured with calipers twice weekly. Tumors were allowed to grow up to 100 mm^3 prior to treatment. Mice were randomized and either 240 µg of QUAD-DM1 (12 mg/kg) or PBS was injected intravenously (IV) into the tail vein. Mice were treated weekly starting on day 0. Mice were euthanized on day 24. $p<0.015$; paired T-test (Prism GraphPad).

Intracranial tumors

Nu/nu mice were intracranially stereotactically injected with 200,000 MDA-MB-231-BrM-luc-RFP cells. Seven days after injection, and after verification of tumor growth, mice were once intracranially infused with QUAD-DM1 conjugate or unconjugated QUAD + DM1 mixture, as in ref. **37**. Three times per week, mice were intraperitoneally injected with 150 mg/kg D-luciferin (Gold Biotechnology, St Louis MO, cat# LUCK-5 g) and imaged using the in vivo Imaging System (Perkin Elmer, Shelton, CT); ($p<0.05$).

Immunohistochemistry

Immunohistochemistry on paraffin slides and tissue microarrays containing human primary breast cancer, lymph node metastasis and metastasis to the brain were performed (TissueArray.com LLC and Tumor Tissue Pathology Core of AHWFB-CCC), as previously described [32]. Slides were stained for EphA2 (Novus-Bio, Centennial, CO, cat# NBP2-24,489 1:200), EphA3 (Genetex, Irvine, CA, cat# GTX114067, 1:200), EphB2 (R&D Systems, Minneapolis, MN, cat# AF467, 2 µg/ml) and IL-13RA2 (made in house, 0.5 µg/ml). Slides were digitally scanned in the Virtual Microscope Core Lab of

AHWFB-CCC. When specimens collected at AHWFB were used, the study was performed under institutional IRB approval: IRB 0000008427. Surgical consent contains provision for use of remnant tissue.

Immunohistochemical staining was scored by a board-certified pathologist (Dr. Ryan T. Mott) using a semi-quantitative approach based on the intensity and proportion of cell staining: 0, 1+, 2+, and 3+. A score of 0 indicates no detectable staining, while a score of 1+ represents weak staining in any proportion of cells. A score of 2+ indicates moderate staining in a majority (> 50%) of cells, and a score of 3+ represents strong staining in a vast majority (> 90%) of cells. The expression pattern was principally cytoplasmic for all four receptors. In cases of heterogeneous staining, the predominant staining intensity was used for scoring.

Immunofluorescence

Frozen sections of breast metastasis to the brain were fixed with acetone, washed with PBS, and blocked with Superblock (Scytek, Logan UT, cat# AAA125). Multicolor staining was performed as previously described [32]. Antibodies included EphA3 (Genetex), EphA2 (R&D Systems cat# AF3035) and IL-13RA2 (made in house). Images were acquired on an Olympus IX70 microscope with a DP80 camera and were processed with Olympus LS cellSens software.

Internalization of QUAD-DM1

1×10^4 cells per treatment were grown overnight on sterile round coverslips. Media was replaced containing 2.0 µg QUAD-DM1 conjugate after 24 h. After 4-h incubation at 37 ^{0}C, cells were fixed in formalin and permeabilized with 0.1% TritonX-100. Monoclonal anti-DM1 antibody (HUABIO, Woburn, MA cat# HA600013, 1:2000) was added and incubated for 1 h at RT. Coverslips were washed with PBS/TritonX-100 prior to addition of Alexa Fluor conjugated secondary antibodies. After 1 h incubation, coverslips were washed and mounted on slides with FluorMount-G with DAPI (Southern Biotech, Birmingham, AL, cat# 0100–20). Images were acquired as above.

Statistical methods

To compare the QUAD (EphA2, EphA3, EphB2, and IL-13RA2) detection rate vs the Hormone (ER, PR, HER2) detection rate we performed two statistical analyses.

The first analysis was to determine for each sample whether the QUAD method, the Hormone method, both methods, or neither method had a detectable level of output.

Thus, for example, for the 50 Breast samples (Fig. 5), each sample was identified as a Yes/No for QUAD and Hormone uptake. Using this data, we then performed a McNemar's test to determine whether there was a significant difference in the uptake proportion between the methods. Next, we assigned two scores to each of the samples, where the QUAD score was the average QUAD uptake (sum of QUAD values divided by 4, (EphA2, EphA3, EphB2, IL-13RA2)) and the Hormone score was the average Hormone update (sum of Hormone values divided by 3 (ER, PR, HER2). We then estimated the difference between the QUAD score and Hormone score for each sample and performed a paired t-test to determine if there was a difference in the average uptake scores between the methods. Finally, we examined the EphA3 component of the QUAD score separately to determine whether this one component was significantly better in detecting uptake than any of the other 3 QUAD components or 3 Hormone components. To do this, we calculated average differences in uptake scores between the EphA3 value and each of the other 6 methods and performed paired t-tests comparing these values.

Animals were used according to the standards set by the institutional animal care and use committee under approval No A21-087 (AHWFB).

Results

We demonstrate here: (i) construction of QUAD-DM1, a drug conjugate analyzed in our experiments, (ii) cytotoxic activity of QUAD-DM1 conjugate on breast cancer cells, (iii) presence of target receptors for QUAD in breast cancer cells using western blots and flow cytometry; (iv) internalization of QUAD-DM1 by cells overexpressing the four targeted receptors, (v) defined cell cycle changes in response to QUAD-DM1, (vi) specificity of QUAD-DM1 targeting in a competition binding experiments, (vii) production of T-DM1 (trastuzumab emtansine) in-house, which is directed against HER-2 receptor, and comparison with our QUAD-DM1, (viii) in vivo anti-tumor experiments using non-optimized dose of the QUAD-DM1 in mice carrying MDA-MB-231 tumors in mammary fat pad and mice with MDA-MB-231-BrM tumors growing intracranially, (ix) immunohistochemistry on sections of breast cancer brain metastases for immunoreactive EphA2, EphA3, EphB2 and IL-13RA2 target receptors, (x) gene expression of *ephA2*, *ephA3*, *ephB2* and *il-13ra2* in TCGA breast cancer data set, (xi) tissue microarrays for the EphA2, EphA3, EphB2 and IL-13RA2 target receptors in primary breast cancer and also lymph nodes, (xii) specificity of QUAD-DM1 targeting by avid binding to the EphA3 receptor, (xiii) staining of breast cancer brain metastasis for immunoreactive EphA2, EphA3 and IL-13RA2.

The QUAD-DM1 drug conjugate was constructed, produced and then tested (Figs. 1 and 2). The drug conjugate

(Fig. 2A) was highly cytotoxic to the breast cancer cell lines MDA-MB-231, MDA-MB-231-BrM, HCC1806 and BT549 (Fig. 2B). The killing effect of QUAD-DM1 was time-, and targeted receptors-dependent, which was increased with the length of incubation from 24 to 72 h (Additional File 1). This was suggestive that the breast cancer brain metastases may also express receptors targeted by the QUAD ligand. Thus, we performed Western blots for the targeted receptors in BT549, HCC1806, MDA-MB-231, MDA-MB 231-BrM, MDA-MB-468, and T47D cells. Specific immunoreactive receptors were variable (Fig. 2C). The EphA3 receptor was highly present in HCC1806, MDA-MB-231, and MDA-MB-231-BrM cells while HC1806 and MDA-MB-468 cells were enriched in the EphB2 receptor (Fig. 2C). The BT549 cells had a low level of the QUAD receptors by immunoblotting, similarly to T47D cells, and they responded rather poorly to QUAD-DM1 (Fig. 2C). Of interest, IL-13RA2 was highly over-expressed in MDA-MB-231-BrM breast cancer brain metastatic cells (Fig. 2C). In comparison with paclitaxel [35] and capecitabine [36] anti-breast cancer chemotherapeutics, MDA-MB-231 and MDA-MB-231-BrM cells responded in a similar fashion (Additional File 2 A). Paclitaxel exhibited killing activity at more than 10^{-8} M while capecitabine was completely inactive on these cells up to 10^{-7} M concentration (Additional File 2 A).

We also performed flow cytometry. All six tested cell lines demonstrated the presence of targeted receptors for QUAD (Fig. 2D). Next, we tested whether QUAD or QUAD-DM1 induces changes in cell cycle. We found that only the cells treated with QUAD-DM1 conjugate underwent cell cycle arrest in G2 phase (Fig. 2E). This agrees with the previously observed effects of DM1 [38]. In addition, we detected that Histone H3 pSer10 [39] is maintained in QUAD-DM1 treated breast cancer cells. It reflects the fact that cells reached metaphase but are not able to complete cell division (Fig. 2F and Additional File 2B). Aurora A [40] was also highly present in response to QUAD-DM1 (Fig. 2F and Additional File 2B) reflecting the fact that cells reached G2/M phase but did not complete mitosis. We observed a sustained upregulation of PLK-1 in response to QUAD-DM1, confirming G2/M cell cycle arrest [41] (Fig. 2F and Additional File 2 C). Apoptotic death for PARP cleavage and caspase 3 cleavage could not be detected for MDA-MB-231 and MDA-MB-231-BrM cells treated with 1 nM QUAD-DM1 at 24- and 48- hour time points (data not shown). We also documented that QUAD-DM1 is internalized by QUAD receptors-enriched MDA-MB-231-BrM cells, but not by T47D cells with marginal presence of these receptors (Additional File 3).

To further document the specificity of the QUAD-DM1 targeting breast cancer cells, we added 200 nM of unconjugated QUAD, which very effectively (~, or > 3 logs) blocked the action of QUAD-DM1 (Fig. 3A). Furthermore, we have produced T-DM1 (trastuzumab emtansine) in-house, which is directed against HER-2 receptors, and compared with our QUAD-DM1 (Fig. 3B-C). The IC_{50} of QUAD-DM1 ranged between 10^{-11} to 10^{-8} M on MDA-MB-231, while T-DM1's IC_{50} was between 10^{-10} and 10^{-7} M on all four cell lines tested (Fig. 3C). Only the HER2 expressing SK-Br-3 breast cancer cells responded somewhat better to T-DM1 than QUAD-DM1 (Fig. 3C-D). Noteworthy, our results with T-DM1 are equal or even better than the ones reported in the literature [38]. We have also analyzed the four receptors immunoreactivity, and that of HER2, in the four breast cancer cell lines: MDA-MB-231, MDA-MB-231-BrM, SK-BR3, and ZR-75 (Fig. 3D). MDA-MB-231 and MDA-MB-231-BrM cells expressed jointly all four receptors at various levels. Noteworthy, MDA-MB-231-BrM cells were high over-expressors of the IL-13RA2 (Fig. 3D). Next, we performed an in vivo anti-tumor experiment using non-optimized dose of the conjugate in mice carrying MDA-MB-231 tumors in the fourth mammary fat pad. The dose was approximately 4 × higher than the one used for Kadcyla [42]. The systemic treatment produced significant anti-tumor activity with no noticeable toxicity (Fig. 3E). In another model, we treated mice bearing MDA-MB-231-BrM tumors growing intracranially with

(See figure on next page.)

Fig. 2 **A** SDS-PAGE of QUAD (lane 1) and its QUAD-DM1 conjugate (lane 2). **B** Cell viability assay of QUAD-DM1 conjugate on five breast cancer cell lines, including a pair of primary and metastatic tumors (MDA-MB-231 and MDA-MB-231-BrM). The IC_{50}s of QUAD-DM1 for the cell killing is shown in the accompanying table. One breast cancer cell line, the BT549 cells, was less responsive to QUAD-DM1. These cells do not express QUAD receptors (not shown), and any cytotoxicity observed is likely dependent on the action of DM1 rather than through targeting by the QUAD ligand. **C** Western blot analysis of target receptors in established breast cancer cell lines. Primary antibodies included EphA3 (MyBiosource), EphA2 (clone D7 made in house), EphB2 (R&D Systems) and IL-13RA2 (HUABIO). Molecular weights of the proteins are as follows: EphA3, 110,131 Da; EphA2, 108,266 Da; EphB2, 117,493 Da; and IL-13RA2, 44,176 Da. All four proteins are glycosylated hence molecular weights in Western blots are higher than predicted from the primary sequence. **D** Flow cytometry for QUAD in human breast cancer cell lines. The red line corresponds to QUAD and the black line represents isotype control. **E** QUAD-DM1 causes cell cycle arrest in G2 phase. Data was analyzed with FCS Express using multicycle DNA analysis. **F** Cellular events in response to QUAD-DM1. QUAD-DM1 caused sustained histone H3 Ser-10 phopshorylation, Aurora A expression and PLK-1 expression

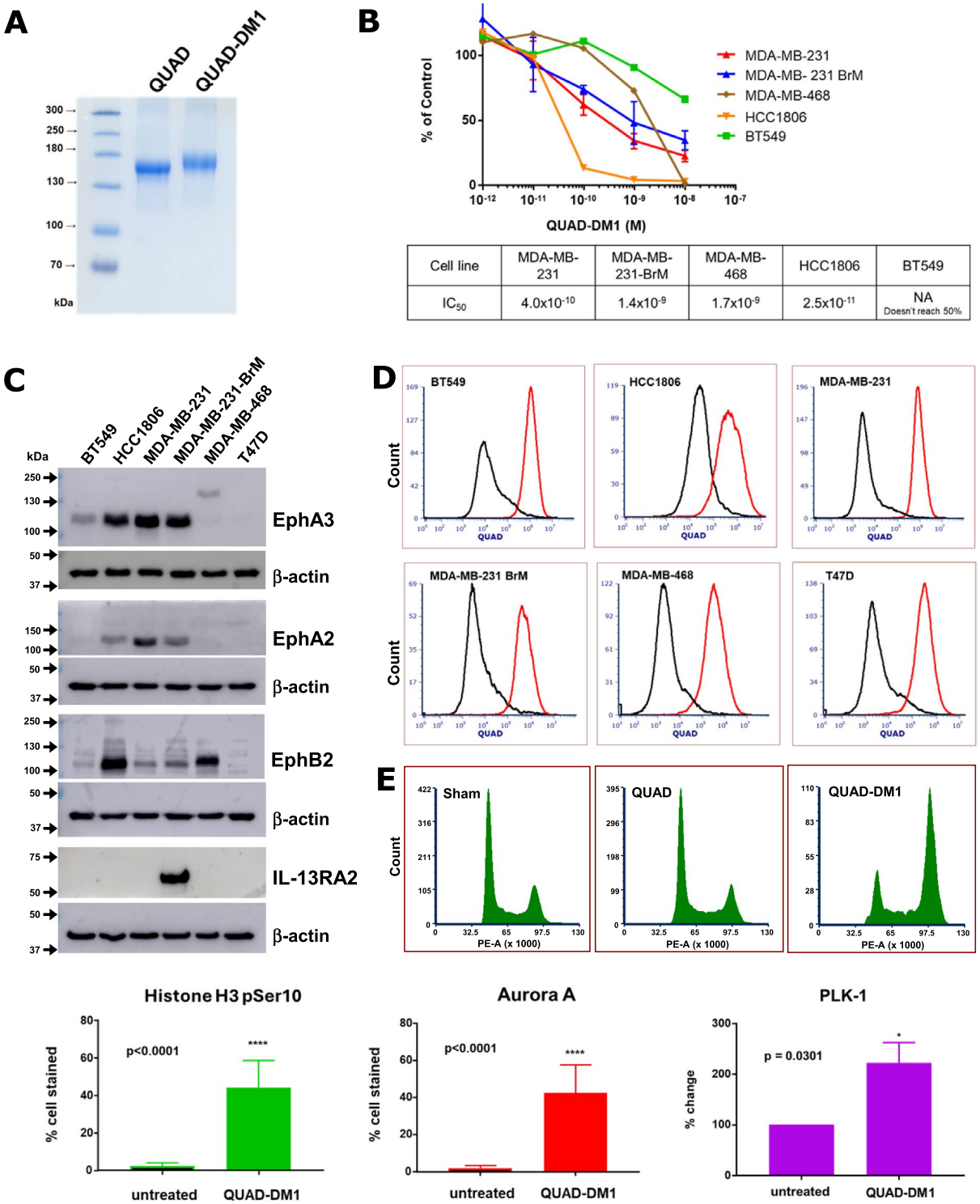

Cell line	MDA-MB-231	MDA-MB-231-BrM	MDA-MB-468	HCC1806	BT549
IC_{50}	$4.0x10^{-10}$	$1.4x10^{-9}$	$1.7x10^{-9}$	$2.5x10^{-11}$	NA Doesn't reach 50%

Fig. 2 (See legend on previous page.)

QUAD-DM1 conjugate administered loco-regionally (Fig. 3F). Again, using a non-optimized dose of the conjugate, we observed significant tumor growth inhibition while the solvent (PBS) or unconjugated QUAD + DM1 mixture lacked anti-tumor action at the corresponding concentrations (Fig. 3E-F). The growth of tumors and response to therapy were monitored by bioluminescent reading of IC tumor bearing mice (Fig. 3G).

To further document the in situ presence of the studied receptors, immunohistochemistry was performed for the target receptors (Fig. 4). EphA2, EphA3 and IL-13RA2 were prominently stained while EphB2 receptor stained to a lesser degree in the specimens of primary breast cancer and patient matched breast cancer brain metastases (Fig. 4A). Control staining for the studied specimens is shown in Additional File 4. In another set of five breast cancer brain metastases, the staining for the target receptors was clearly present (Fig. 4B). The ten samples evaluated in Fig. 4A contained the sections of TNBC and of triple-positive (ER, PR, and HER2) (only one tumor) matched primary tumors and metastases, and they demonstrated readily detectable expression levels of IL-13RA2, EphA3 and EphA2 receptors, and less so for the EphB2 receptor (Fig. 4C). On average, brain metastases expressed the four studied receptors at lower levels than the primary breast cancers, but only one brain metastasis did not express any of the four target receptors in this studied group (Fig. 4C).

Of the 10 samples where both QUAD and Hormone data were available (see Methods section), the QUAD method identified all 10 whereas the Hormone method identified 6 of the samples. The McNemar's test for comparing the agreement between methods had a Chi-Square value of 4 ($p = 0.125$). So, while this was statistically non-significant, the sample size was low ($n = 10$), and the comparison of the rate of detection between groups was 100% (QUAD) vs 60% (Hormone). When comparing the average QUAD Score vs. the average Hormone score, we found the average QUAD Score was 1.28 vs the average Hormone score was 0.37 (difference was 0.91). The paired t-test indicated that the QUAD score was significantly higher ($t = 5.37$, $p < 0.0005$) than the Hormone score. When examining the EphA3 marker vs all other markers, we found that the average EphA3 marker score was 2.10 and was found on all 10 Breast (primary) samples. This score was significantly higher than all the other individual QUAD markers except for the IL-13RA2 marker (mean 1.2, $p = 0.054$ when compared to EphA3). The EphA3 marker had a significantly higher marker score than all the Hormone markers ($p < 0.001$ for all comparisons).

Of the 10 samples where both QUAD and Hormone data were available, the QUAD method identified 9 (90%) of the samples whereas the Hormone method identified 6 of the samples. The McNemar's test for comparing the agreement between methods had a Chi-Square value of 0.18 ($p = 0.375$). This was the first example where the QUAD score did not identify a sample where the Hormone score did. So, there were 5 samples where both methods had a positive score, 4 samples where only the QUAD score was positive and one sample where only the Hormone score (Sample 4; Fig. 4C) was positive. When comparing the average QUAD Score vs. the average Hormone score, we found the average QUAD Score was 1.00 vs the average Hormone score was 0.37 (difference was 0.63). The paired t-test indicated that the QUAD score was significantly higher ($t = 3.68$, $p = 0.005$) than the Hormone score. When examining the EphA3 marker vs all other markers, we found that the average EphA3 marker score was 1.30 and was found on eight of the Breast (Brain Met) samples. This score was significantly higher than the EphB2 marker ($t = 2.54$, $p = 0.3$) and two of the Hormone markers (ER, $t = 2.86$, $p = 0.0187$ and PR, $t = 3.97$, $p = 0.003$).

We next composed heatmaps for the gene expression of the target receptors in TCGA breast cancer data set. We analyzed all breast cancers, TNBC, and HER2-negative breast cancers as separate groups (Fig. 5A). In all cases, the gene expression for *ephA2* and *ephB2* were the highest with the lesser *ephA3* expression and *il-13ra2* as the least expressed gene, with somewhat more presence in TNBC. The results presented here are in whole or part based upon data generated by the TCGA Research Network (https://www.cancer.gov/tcga).

(See figure on next page.)

Fig. 3 In vitro and in vivo properties of QUAD-DM1. **A** Specificity of QUAD-DM1 killing action on breast cancer cells. 200 nM of unconjugated QUAD was added at each concentration of QUAD-DM1. **B** Western blot of QUAD (1), QUAD-DM1 (2), biosimilar Trastuzumab (3) and Trastuzumab-DM1 (T-DM1) (made in house) (4). **C** QUAD-DM1 and in-house made T-DM1 cytotoxicity in breast cancer cell lines. The IC_{50}s of QUAD-DM1 for the cell killing is included in the table. **D** Western blot analysis of 4 QUAD receptors and HER2 in cells treated with T-DM1. **E** Anti-tumor activity of QUAD-DM1 in MDA-MB-231 breast cancer tumors growing in mammary pads ($n = 5$). $p < 0.015$; paired T-test (GraphPad Prism). **F** Anti-tumor activity of QUAD-DM1 in MDA-MB-231-BrM breast cancer tumors growing in brain ($n = 5$); $p < 0.05$; two-tailed test up to day 13 (GraphPad Prism). For the control treatment, we used a 1:2 molar ratio of unconjugated QUAD + DM1 mixture. This equated to 4 µg QUAD and 70 ng (0.07 µg) DM1-SMCC per mouse to simulate the molar ratio in our conjugate. **G** Representative anti-tumor response to QUAD-DM1 in mice with intracranial tumors. Time course of bioluminescent images of IC tumor bearing mice pre- and post-treatment with QUAD-DM1 is shown

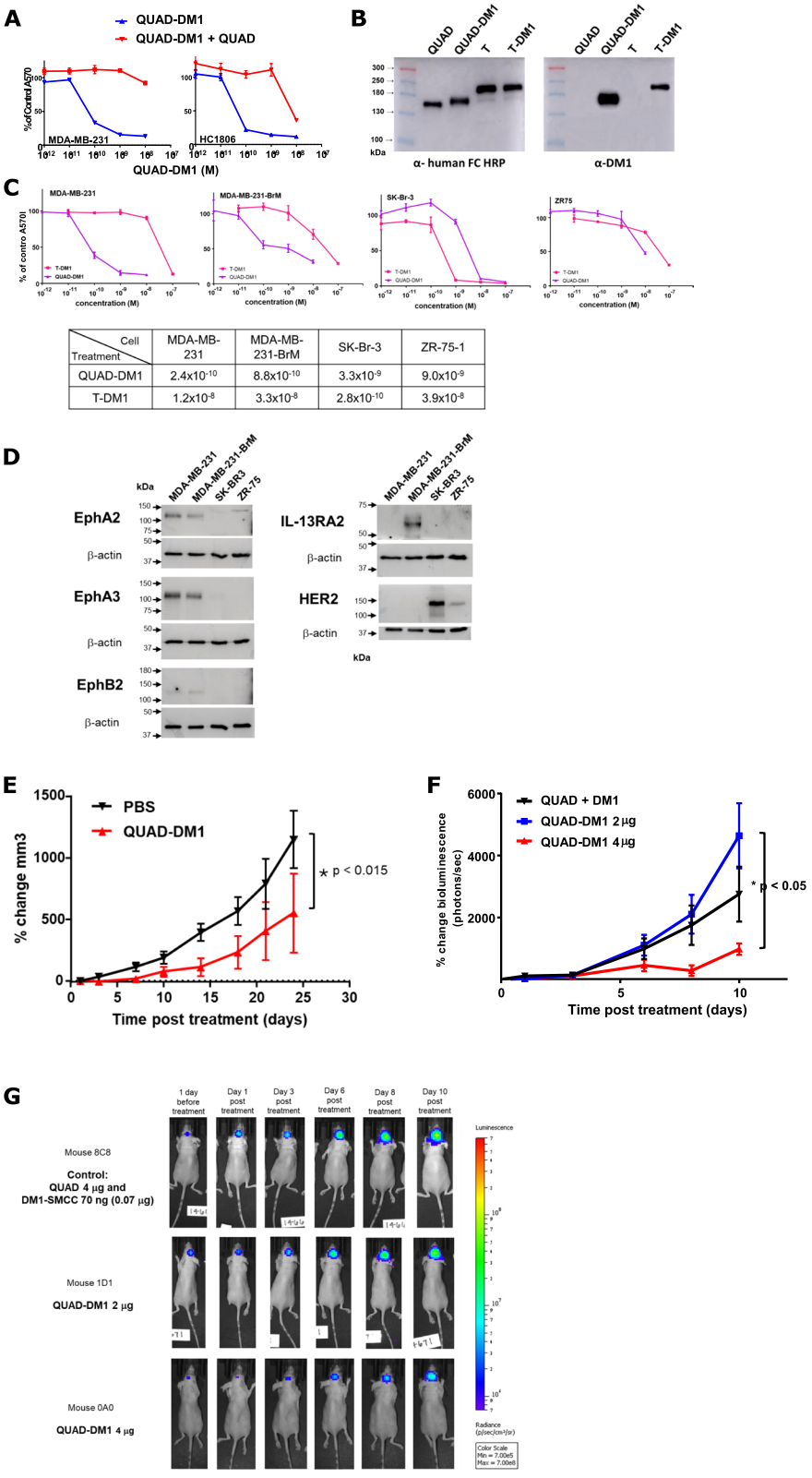

Cell / Treatment	MDA-MB-231	MDA-MB-231-BrM	SK-Br-3	ZR-75-1
QUAD-DM1	$2.4x10^{-10}$	$8.8x10^{-10}$	$3.3x10^{-9}$	$9.0x10^{-9}$
T-DM1	$1.2x10^{-8}$	$3.3x10^{-8}$	$2.8x10^{-10}$	$3.9x10^{-8}$

Fig. 3 (See legend on previous page.)

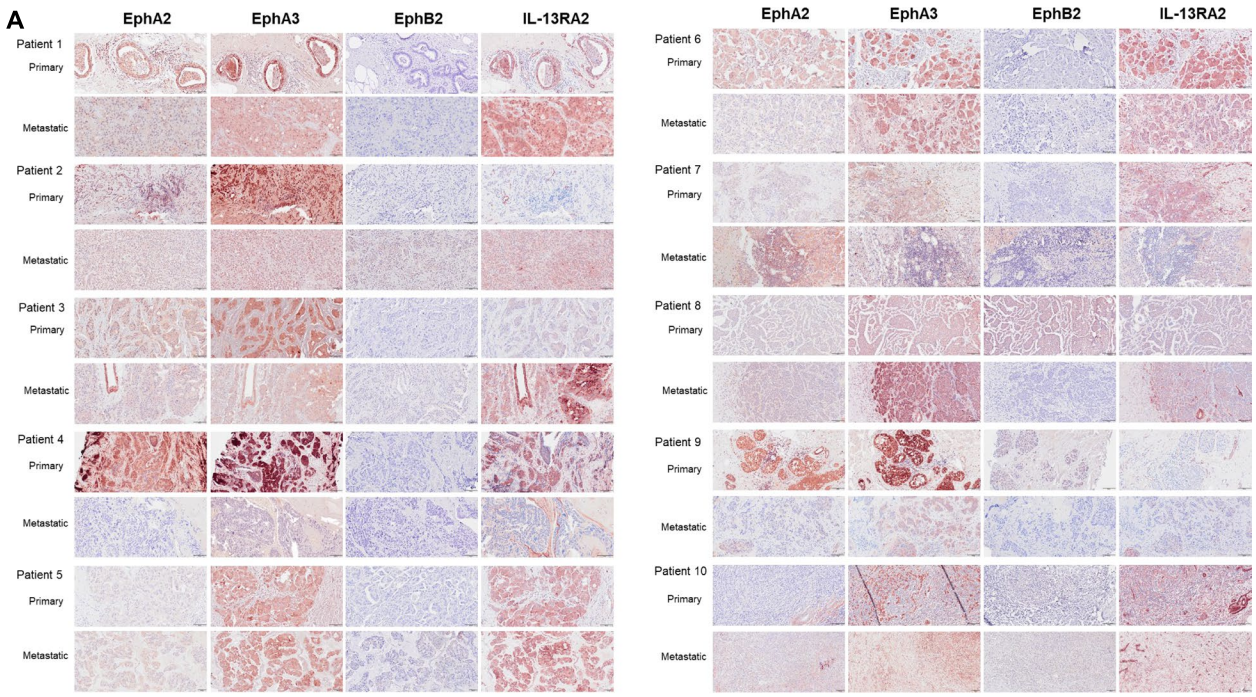

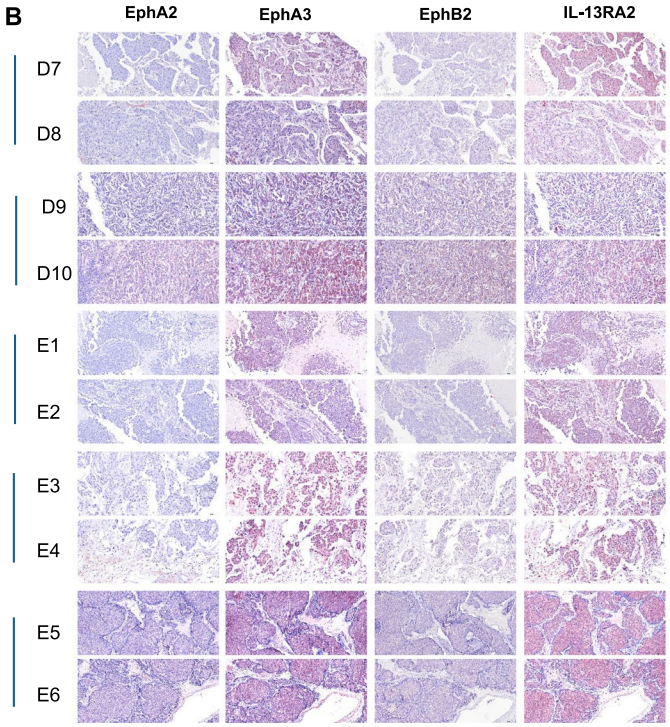

C

	Breast cancer	EphA2	EphA3	EphB2	IL-13RA2	ER	PR	HER2
1	primary	1+	2+	-	2+	-	-	-
1	brain met	1+	1+	-	2+	-	-	-
2	primary	1+	3+	-	-	+	+	+
2	brain met	1+	1+	1+	2+	+	+	+
3	primary	1+	2+	-	-	-	-	+
3	brain met	1+	1+	1+	2+	-	-	+
4	primary	3+	3+	-	3+	+	-	+
4	brain met	-	-	-	-	+	-	+
5	primary	1+	2+	-	2+	+	-	+
5	brain met	2+	2+	-	2+	+	-	+
6	primary	2+	2+	1+	2+	-	-	+
6	brain met	1+	1+	-	1+	-	-	+
7	primary	1+	1+	-	1+	-	-	-
7	brain met	3+	-	1+	-	-	-	-
8	primary	2+	2+	2+	1+	+	+	-
8	brain met	2+	3+	-	-	+	+	-
9	primary	3+	3+	-	-	-	-	-
9	brain met	2+	2+	-	1+	-	-	-
10	primary	-	1+	-	1+	-	-	-
10	brain met	-	2+	-	1+	-	-	-

Fig. 4 Expression of the four target receptors in breast cancer primary tumors and breast cancer metastases to brain (**A**). Control staining is shown in Additional File 4. **B** Immunohistochemistry of breast cancer metastases to brain. Commercial TMA of multiple metastases to brain: 5 patients/2 cores per patient samples. **C** Histological scoring of IL-13RA2. EphA3, EphA2, and EphB2 staining of ten patient-matched breast cancer and its brain metastasis). Estrogen receptor (ER), progesterone receptor (PR) and HER2 scoring of the samples were obtained from patients' original pathology report following surgery, neurological symptoms or IHC changes. All tissue samples were collected at AHWFB-CCC Tissue Bank

A

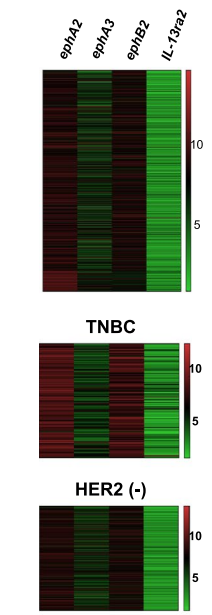

B

Breast	Grade	Stage	EphA2	EphA3	EphB2	IL-13RA2	ER	PR	HER2
1	2	IIB	0	1	0	1	0	0	0
2	2	IIA	1	3	0	2	1	2	0
3	1	IIIB	0	1	0	0	NA	1	0
4	2	IIA	0	3	0	3	NA	3	0
5	2	IA	1	3	1	3	NA	3	0
6	1	IA	1	3	1	2	NA	NA	0
7	1	IIA	0	1	0	1	NA	NA	2
8	2	IIB	0	3	1	2	NA	NA	0
9	1	IIIB	1	3	1	3	NA	2	0
10	1	IIB	0	2	1	2	NA	NA	0
11	2	IIA	2	3	0	3	3	0	0
12	1	IIA	1	3	0	2	0	0	0
13	2	IIA	0	3	0	2	3	0	0
14	2	IIB	0	3	0	1	2	1	0
15	2	IIA	1	3	1	3	0	0	0
16	2	IIA	1	3	0	2	2	1	0
17	2	IIA	0	3	1	2	1	2	0
18	2	IIB	1	3	1	2	0	0	0
19	2	IIA	0	1	0	1	0	0	0
20	2	IIIB	1	3	0	2	1	0	0
21	2	IIA	3	3	1	2	2	0	3
22	2	IIB	0	1	0	0	0	0	0
23	3	IIA	1	2	0	1	1	0	0
24	2	IA	0	3	0	2	3	3	0
25	2	IIIB	1	3	1	2	0	0	3
26	2	IIA	1	3	1	2	0	0	3
27	2	IIB	1	3	0	3	3	0	3
28	2	IIA	0	2	0	1	0	0	0
29	2	IIA	1	3	1	3	3	3	0
30	2	IIIA	1	2	1	2	1	2	0
31	1	IIA	2	3	1	2	0	0	2
32	3	IA	0	1	0	1	1	0	0
33	3	IIA	0	1	0	0	1	0	0
34	2	IIA	1	3	1	3	3	3	0
35	3	IIA	1	3	0	3	1	0	0
36	1	IIA	0	2	0	1	0	0	3
37	2	IIA	0	3	0	1	0	0	2
38	2	IIA	1	3	1	2	3	0	0
39	2	IIA	1	2	0	1	2	3	0
40	2	IIA	1	2	1	2	0	0	0
41	3	IIIB	1	2	1	1	0	0	3
42	3	IIA	1	3	1	2	0	0	0
43	3	IIA	1	3	1	2	1	0	0
44	3	IIA	0	1	0	0	0	0	0
45	3	IIB	1	3	1	2	0	0	3
46	-	IIIC	2	3	1	1	0	0	0
47	2	IIA	0	3	1	3	3	3	0
48	-	IIB	0	1	0	1	0	0	0
49	-	IIB	0	3	0	3	2	0	0
50	-	IIA	0	3	0	3	2	0	0

C

Lymph nodes	EphA2	EphA3	EphB2	IL-13RA2	ER	PR	HER2
1	2	3	1	2	0	0	3
2	0	3	0	3	0	0	3
3	0	2	0	1	2	1	0
4	0	0	0	1	0	0	0
5	1	3	1	2	0	0	3
6	0	3	1	3	2	1	0
7	0	3	1	3	0	0	3
8	0	3	0	2	3	3	0
9	1	3	1	2	NA	NA	*
10	0	1	0	3	0	0	0
11	1	3	0	3	0	0	0
12	1	3	1	2	0	0	3
13	1	3	0	1	3	0	0
14	0	1	0	2	1	1	0
15	2	3	1	3	3	0	0
16	1	1	1	0	3	1	0
17	0	2	0	2	0	0	3
18	0	2	0	1	0	0	0
19	1	3	1	3	0	0	2
20	1	3	0	3	2	0	3
21	1	3	0	2	0	0	0
22	1	2	0	1	3	1	3
23	0	1	0	1	3	0	0
24	1	3	1	2	0	0	3
25	0	3	1	3	0	0	0
26	0	1	0	1	0	0	3
27	0	1	0	1	2	3	0
28	1	3	1	2	NA	NA	*
29	0	2	0	3	3	2	0
30	1	3	0	3	0	0	0
31	0	2	0	2	0	0	0
32	2	3	1	2	3	NA	0
33	0	3	0	3	NA	NA	0
34	0	1	0	0	NA	NA	0
36	0	2	1	2	NA	NA	0
36	0	2	0	2	NA	NA	0
37	0	2	0	3	NA	NA	0
38	0	2	0	2	NA	0	0
39	0	2	0	3	NA	0	0
40	1	3	1	3	2	1	0

Fig. 5 Gene expression of the four target receptors. **A** Heatmap of gene expression of *epha2, epha3, ephb2* and *il-13ra2* in TCGA breast cancer data set. The data for all types and triple negative and HER2 negative breast cancer are presented. The results shown here are in whole or part based upon data generated by the TCGA Research Network (https://www.cancer.gov/tcga). **B** Breast carcinoma TMA containing single core per case. Staining for the target receptors included 50 cases of primary breast cancer with 46 cases of invasive carcinoma of no special type, 1 neuroendocrine carcinoma, and 3 medullary carcinomas. Tissue was scored for staining intensity by a neuropathologist at AHWFB (Dr. Ryan T. Mott) on a scale of 0–3 (see also Additional File 5 A). **C** Lymph nodes TMA containing single core per case. Score is 0 to 1 +, HER2-negative; score 2 +, borderline or equivocal; score 3 +, HER2-positive

We then analyzed tissue microarrays for four target receptors in primary breast cancer and lymph nodes (Fig. 5B-C and Additional File 5). We found that less than 20% of specimens were HER2-positive while there was not a negative specimen for the expression of the four receptors under study, and only three specimens were positive for just one receptor (Fig. 5B, and Additional File 5). Thus, the four target receptors are highly expressed in primary breast cancer (Fig. 5B) and lymph node metastases (Fig. 5C) (50 and 40 specimens examined, respectively) with marginal staining found in "normal" adjacent tissue (Additional File 5B). The specificity of QUAD-DM1 targeting was further supported by avid binding to the EphA3 receptor and null binding to PDL1 and CD80 (Additional File 6), and no IC_{50} detected on HUVEC endothelial cells treated with QUAD-DM1, up to 10^{-8} M (data not shown). In addition, human eA5 interacts with the EphA3 receptor in a species-crossed manner, which makes studies in mice more relevant to human situation (Additional File 7).

In statistical analysis, of the 50 samples, the QUAD method (see Methods section) identified all 50 whereas the Hormone method identified 35 of the samples. The McNemar's test for comparing the agreement between methods had a Chi-Square value of 15 ($p < 0.0001$). When comparing the average QUAD Score vs. the average Hormone score, we found the average QUAD Score was 1.36 vs the average Hormone score was 0.69 (difference was 0.66). The paired t-test indicated that the QUAD score was significantly higher ($t = 6.95$, $p < 0.0001$) than the Hormone score. When examining the EphA3 marker vs all other markers, we found that the average EphA3 marker score was 2.48 and was found on all 50 breast samples. This score was significantly higher than any of the other individual QUAD or Hormone markers ($p < 0.0001$ for all comparisons).

Of the 38 samples where both QUAD and Hormone data were available, the QUAD method identified all 38 whereas the Hormone method identified 23 of the samples (Fig. 5C). The McNemar's test for comparing the agreement between methods had a Chi-Square value of 15 ($p < 0.0001$). When comparing the average QUAD Score vs. the average Hormone score, we found the average QUAD Score was 1.31 vs the average Hormone score was 0.71 (difference was 0.58). The paired t-test indicated that the QUAD score was significantly higher

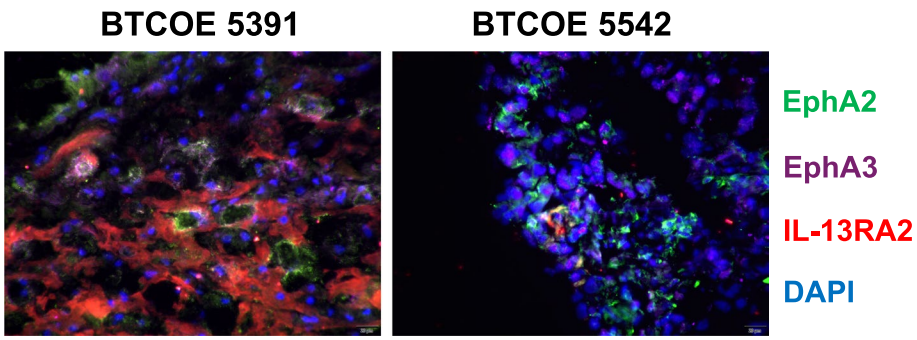

Fig. 6 Immunoreactive EphA2, EphA3 and IL-13RA2 in brain metastatic breast cancer. Complementary and overlapping expression of EphA2, EphA3 and IL-13RA2 in breast metastatic cancer by immunofluorescence. Almost all cells stained for one of the tested three receptors. BTCOE 5391 is HER2 + and BTCOE 5542 represents TNBC

(t = 4,38, $p < 0.0001$) than the Hormone score. When examining the EphA3 marker vs all other markers, we found that the average EphA3 marker score was 2.30 and was found on all 40 lymph node samples. This score was significantly higher than all the other individual QUAD markers except for the IL-13RA2 marker (mean 2.08, $p = 0.08$ when compared to EphA3). The EphA3 marker had a significantly higher marker score than all the Hormone markers ($p < 0.001$ for all comparisons).

We also stained the sections of breast cancer brain metastasis for immunoreactive EphA2, EphA3 and IL-13RA2 (Fig. 6). Complementary and overlapping expressions of EphA2, EphA3 and IL-13RA2 in breast cancer by immunofluorescence were observed. Almost all cells stained for one of the three examined receptors. We stained HER2-positive and TNBC specimens as examples (Fig. 6).

Discussion

Our study demonstrates that breast cancer and related brain metastasis are over-expressors of EphA2, EphA3, EphB2 and IL-13RA2 receptors. The four receptors can be targeted concomitantly by a ligand termed QUAD. The receptors' overexpression was documented using a variety of approaches that include gene and protein expression analyses, immunostaining, and responsiveness to a targeted drug conjugate. The conjugate also produced an anti-tumor effect in two in vivo models of tumors. This represents a very encouraging finding of a new set of targets for the development of precision approaches to treat breast cancer and related brain metastasis.

To demonstrate the presence of the target receptors in breast cancer, we have analyzed tissue microarrays of primary breast cancer and lymph nodes. As expected, less than 20% of specimens were seen as HER2-positive while there was not a specimen negative for the expression of the examined four target receptors, and only three specimens were positive for just one receptor. Thus, the target receptors for QUAD are highly expressed in primary breast cancer and associated lymph nodes further confirming that they are excellent targets for therapies of almost all breast cancer subtypes. Vast majority of breast tumor specimens, regardless of whether it was a primary tumor or its metastasis, have stained for the IL-13RA2, EphA2 and EphA3, and less for the EphB2 receptor. Of importance, the same specimens, as analyzed by a clinical laboratory at AHWFB, showed much less prevalence of staining for HER2 and ER, and even less so for the PR than for the four target receptors. Only one brain metastasis of breast cancer archived at AHWFB did not express any of the target receptors.

To make a targeted therapeutic conjugate, we used DM1, a microtubule-disrupting agent. This agent is used for conjugation with Herceptin to produce trastuzumab emtansine (T-DM1), Kadcyla, a newer generation anticancer drug [42]. The IC_{50} for the QUAD-DM1 conjugate reaches the low picomolar range. QUAD-DM1 was ~ 50 times more potent than all other QUAD-based drug conjugates tested [33, 43, 44]. In addition, in our further toxicity studies, we could inject up to 15 mg/kg QUAD-DM1 (data not shown) while T-DM1 can be given clinically at less than 3 mg/kg. Pre-clinical studies with T-DM1 utilized mice [33] while Trastuzumab does not interact with murine HER2 receptor. This complicates a direct preclinical comparison of the two conjugates. Furthermore, T-DM1 diminishes recurrence and death of patients with invasive breast cancer [42], but 80% of breast cancer patients do not express the target. Clearly, novel drugs are needed to be available to larger group of patients. In addition, the modified IL-13 and eA5 receptor ligands of human origin that are included in our constructs [13, 14] are fully reactive with the canine and mouse receptors,

as reported previously for IL-13RA2 [32, 37], and documented further in binding, flow cytometry, cytotoxicity and functional assays for the canine/murine Eph receptors interaction with human eA5 (e.g., Additional File 7). Thus, it is expected that QUAD-DM1 should be well tolerated for human application.

It is possible that tumor sites could lose some targeted receptors during therapy with QUAD-DM1. Breast tumors, like other cancers, undergo profound genomic changes due to treatment pressures [38, 45, 46] but whether this takes place during QUAD-DM1 treatment remains to be seen. Our four-pronged approach should allow sustained activity in evolving tumors and in fact address, at least in part, tumor heterogeneity. Continuous effects were observed clinically with concomitant targeting of more than one receptor [47, 48]. We have observed a similar therapeutic effect in dogs with spontaneous brain tumors treated with a cocktail of two targeted cytotoxins [32].

Our goal is to develop an effective way to target breast cancer and related brain metastases. The only verification of such a goal will be the performance of clinical trials in patients. We have developed a potent and specific anti-cancer drug conjugate, QUAD-DM1, which targets several tumor-associated receptors simultaneously. This allowed for targeting of almost entire tumors in vast majority of patients.

Conclusions

Triple negative breast cancer and related brain metastases represent an area in medicine greatly in need of effective therapies. We have identified a new set of widely expressed target receptors in these disease conditions, represented by a group of four transmembrane receptors: EphA2, EphA3, EphB2 and IL-13RA2. A drug conjugate targeting these four target receptors, QUAD-DM1, demonstrated significant tumoricidal potency in vitro and in vivo. It also has an excellent safety profile when given intravenously or intracranially. Thus, breast cancer and its brain metastasis appear to be excellent targets for QUAD-DM1. We believe that further clinical evaluation of this conjugate is warranted. We envision that the initial studies will be focused on brain metastases and loco-regional delivery of QUAD-DM1, using convection-enhanced delivery, especially in patients with TNBC. However, primary breast cancer should also be considered as potential target for QUAD-DM1 therapy in the future. It is difficult to predict whether QUAD-DM1 given systemically would have any effect on brain metastases. Considering the size of the QUAD-DM1 conjugate, we presume that the drug candidate will not cross readily the blood-tumor barrier, but this possibility may not be entirely excluded due to the changes in microvasculature within the metastatic lesions.

Abbreviations

AA	Amino acid
ATCC	American Type Tissue Collection
AHWFB	Atrium Health Wake Forest Baptist
BMBC	Brain Metastasis of Breast Cancer
BSA	Bovine Serum Albumin
CCC	Comprehensive Cancer Center
DLT	Dose Limiting Toxicity
DM1	Maytansinoid
EPH	Erythropoietin-Producing Hepatoma
ER	Estrogen Receptor
HER2	Human Epidermal Growth Factor Receptor 2
GBM	Glioblastoma
IV	Intravenous
IL-13RA2	Interleukin 13 Receptor Alpha 2
MTT	3-(4,5-Dimethylthiazol-2-yl)-2,5-diphenyltetrazolium bromide
PBS	Phosphate-buffered Saline
PDL1	Programmed Death-ligand 1
PR	Progesterone Receptor
SPDP	Succinimidyl 3-(2-pyridyldithio) Propionate
QUAD	Ligand Binding to four receptors
TAM	Tumor-associated Macrophages
T-DM1	Trastuzumab Emtansine
TNBC	Triple Negative Breast Cancer

Supplementary Information

The online version contains supplementary material available at https://doi.org/10.1186/s13058-025-02100-y.

Additional file 1. Cytotoxicity of QUAD-DM1 on MDA-MB-231-BrM and HCC1806 breast cancer cell lines. The cytotoxic effect of QUAD-DM1 potentiates with the time of cells treatment. This cytotoxic effect is dependent on the binding of QUAD-DM1 to the Eph receptors through joint eA5, eA1, and eB1 ligand activities.

Additional file 2. Cytotoxic activity of Paclitaxel and Capecitabine on breast cancer cell lines: MDA-MB-231 and MDA-MB-231-BrMand the action of QUAD-DM1 on treated breast cancer cells.Paclitaxel and Capecitabine were used at concentrations up to 10^{-7}M. Only Paclitaxel demonstrated cytotoxic activity in this range. Paclitaxel was equally, or slightly less, active than QUAD-DM1.The expression of Histone H3 pSer10 and Aurora A in response to QUAD-DM1. The secondary antibody for Histone H3 pSer10 is green fluorescence and the secondary antibody for Aurora A is red fluorescence.Immunoreactive PLK-1 in MDA-MB-231 breast cancer cells treated with QUAD-DM1.

Additional file 3. Internalization of QUAD-DM1 in breast cancer cells. MDA-MB-231-BrM cells were treated with 2.0 mg of QUAD-DM1 for 4 hrs. Internalization of QUAD-DM1 was seen in, EphA2, EphA3, EphB2 and IL-13RA2 receptors-enriched MDA-MB-231-BRM cells, but not in these receptors-low cells like T47D. QUAD was detected by anti-human IgG-Alexa Fluor-488 green fluorescence and DM1 was detected by anti-mouse Alexa Fluor-555 red fluorescence. Nuclei were stained with DAPI.

Additional file 4. Staining for QUAD receptors. The isotype controls staining for breast cancer primary (Fig. 5A) and breast cancer metastasis to brain B (Fig. 5B) specimens. Ten different specimens were stained in each group.

Additional file 5. Immunoreactive IL-13RA2, EphA3, EphA2 and EphB2 in breast cancer. Breast Cancer array BR1008b was used from TissueArray. Rows 1-5, breast cancer specimens; rows 6-9, infiltrated lymph nodes; and row 10, adjacent normal tissue. The quantitative summary of staining results is also shown in Fig. 5. Adjacent "normal" lymph nodes four-receptor staining.

Additional file 6. Human eA5 (aa 21-191) with a C-terminal C residue interacts specifically with the EphA3 receptor, but not with the other factors like PDL1 or CD80. QUAD was produced in its native amino acid sequence in insects (A). Glycosylation null IL-13.E13K (19-132) with 4 additional mutations (G4) N to Q produced in HEK or EXPI cells were also tested (B-C). To diminish binding

to the Fc receptors (F5), additional mutations were introduced: L234F, L235E, N297Q – (N-glycan), K322A, and P331S.

Additional file 7. Human eA5 interacts with the EphA3 receptor in a species-crossed manner. ELISA assay of the binding of human eA5 to recombinant murine and human EphA3 receptors.

Additional file 8. Tumor size monitoring.

Additional file 9. Quadruplicate readings of the cell cytotoxicity assay.

Additional file 10. Original SDS-PAGE (Fig. 2A) and Western blots (Fig. 2C and 3B).

Acknowledgements
Samara Hailey assisted with intracranial surgery and imaging experiments. This work is dedicated to Ewa.

Authors' contributions
Listed authors have contributed substantially to one or all three: 1) the conception and design of the study, acquisition of data, or analysis and interpretation of data; 2) drafting of the manuscript or revising it for important content; and 3) figure preparation. WD, corresponding author (wrote the main manuscript), KNF, JR, RTM, KW, AT, DH.

Funding
Research reported in this publication was supported by the National Cancer Institute of the National Institutes of Health under Award Number R01CA256285 issued to the Wake Forest Baptist Comprehensive Cancer Center (WD), and by the funds from the Dallas Swing Fund and Broyhill Family Fund (WD). The content is solely the responsibility of the authors and does not necessarily represent the official views of the National Institute of Health.

Data availability
Data is provided within the manuscript or supplementary information files.

Declarations

Ethics approval and consent to participate
Not applicable.

Consent for publication
No part of the manuscript is under consideration, in press, published, or reported in a scientific journal in the form of manuscript. All authors read and approved the manuscript. All authors consent to publication.

Competing interests
Waldemar Debinski is a co-inventor on several patent applications related to the subject of this manuscript; several of them have been licensed to WPD Pharmaceuticals. Kaitlin N. Fink, Ryan T. Mott, and Kounosuke Watabe have nothing to disclose. John Rossmeisl is a co-inventor on a patent application covering QUAD-DM1 cytotoxin. Alexandra Thomas reports stock ownership: Johnson & Johnson, Gilead Sciences, Bristol Myers Squibb, Pfizer; consulting or advisory role: Genentech, AstraZeneca; Research Funding: Sanofi, Merck (to the institution); royalties. Denise Herpai is a co-inventor on several patent applications related to the subject of this manuscript; several of them have been licensed to WPD Pharmaceuticals.

Author details
[1]Department of Cancer Biology, Wake Forest School of Medicine, Winston-Salem, NC 27157, USA. [2]Department of Neurology and Neurosurgery, Virginia Tech, Blacksburg, VA 24061-0002, USA. [3]Department of Pathology, Atrium Health Wake Forest Baptist Medical Center, Winston-Salem, NC 27157, USA. [4]Department of Biostatistics and Data Science, Wake Forest School of Medicine, Winston-Salem, NC 2715, USA. [5]Duke Cancer Institute, Durham, NC 27710, USA. [6]Department of Cancer Biology, Wake Forest University School of Medicine, Bowman Gray Campus, 1, Medical Center Blvd., Commons bldg., Rm. 209, Winston-Salem, NC 27157, USA.

Received: 3 December 2024 Accepted: 5 August 2025
Published online: 27 October 2025

References

1. American Cancer Society. The breast cancer facts & figures 2024–2025. https://www.cancer.org/research/cancer-facts-statistics/breast-cancer-facts-figures.html.
2. Pareja F, Geyer FC, Marchiò C, Burke KA, Weigelt B, Reis-Filho JS. Triple-negative breast cancer: the importance of molecular and histologic subtyping, and recognition of low-grade variants. NPJ Breast Cancer. 2016;2: 16036.
3. Bianchini G, Balko JM, Mayer IA, Sanders ME, Gianni L. Triple-negative breast cancer: challenges and opportunities of a heterogeneous disease. Nat Rev Clin Oncol. 2016;13(11):674–90.
4. Dent R, Trudeau M, Pritchard KI, Hanna WM, Kahn HK, Sawka CA, Lickley LA, Rawlinson E, Sun P, Narod SA. Triple-negative breast cancer: clinical features and patterns of recurrence. Clin Cancer Res. 2007;13:4429–34.
5. Howlader N, Cronin KA, Kurian AW, Andridge R. Differences in breast cancer survival by molecular subtypes in the United States. Cancer Epidemiol Biomarkers Prev. 2018;27:619–26.
6. Swain SM, Shastry M, Hamilton E. Targeting HER2-positive breast cancer: advances and future directions. Nat Rev Drug Discov. 2023;22(2):101–26.
7. Exman P, Tolaney SM. HER2-positive metastatic breast cancer: a comprehensive review. Clin Adv Hematol Oncol. 2021;19(1):40–50.
8. Debinski W. An immune regulatory cytokine receptor and glioblastoma multiforme: an unexpected link. Crit Rev Oncog. 1998;9:255–68.
9. Debinski W, Gibo DM. Molecular expression analysis of restrictive receptor for interleukin 13, a brain tumor-associated cancer/testis antigen. Mol Med. 2000;6:440–9.
10. Jaén M, Martín-Regalado Á, Bartolomé RA, Robles J, Casal JI. Interleukin 13 receptor alpha 2 (IL13Rα2): expression, signaling pathways and therapeutic applications in cancer. Biochim Biophys Acta (BBA). 2022;1877(5):188802.
11. Wykosky J, Gibo DM, Stanton C, Debinski W. IL-13 receptor alpha-2, EphA2, and Fra-1 as molecular denominators of high-grade astrocytomas and specific targets for combinatorial therapy. Clin Cancer Res. 2008;14:199–208.
12. Wykosky J, Gibo DM, Stanton C, Debinski W. EphA2 as a novel molecular marker and target in glioblastoma multiforme. Mol Cancer Res. 2005;3(10):541–51.
13. Wykosky J, Palma E, Gibo DM, Ringler S, Turner CP, Debinski W. Soluble monomeric ephrinA1 is released from tumor cells and is a functional ligand for the EphA2 receptor. Oncogene. 2008;27:7260–73.
14. Wykosky J, Gibo DM, Debinski W. A novel, potent, and specific ephrinA1-based cytotoxin against EphA2 receptor-expressing tumor cells. Mol Cancer Ther. 2007;6:3208–18.
15. Xu Q, Wilkinson DG. Eph-related receptors and their ligands: mediators of contact dependent cell interactions. J Mol Med. 1997;75:576–86.
16. Kullander K, Klein R. Mechanisms and functions of Eph and ephrin signaling. Nat Rev Mol Cell Biol. 2002;3:475–86.
17. Pasquale EB. Eph receptor signaling casts a wide net on cell behavior. Nat Rev Mol Cell Biol. 2005;6:462–75.
18. Liu F, Park PJ, Lai W, Maher E, Chakravarti A, Durso L, et al. A genome-wide screen reveals functional gene clusters in the cancer genome and identifies EphA2 as a mitogen in glioblastoma. Cancer Res. 2006;66:10815–23.
19. Li X, Wang Y, Wang Y, Zhen H, Yang H, Fei Z, Zhang J, Liu W, Wang Y, Zhang X. Expression of EphA2 in human astrocytic tumors: correlation with pathologic grade, proliferation and apoptosis. Tumour Biol. 2007;28:165–72.
20. Wang LF, Fokas E, Bieker M, Rose F, Rexin P, Zhu Y, et al. Increased expression of EphA2 correlates with adverse outcome in primary and recurrent glioblastoma multiforme patients. Oncol Rep. 2008;19:151–6.
21. Hatano M, Kuwashima N, Tatsumi T, Dusak JE, Nishimura F, Reilly KM, et al. Vaccination with EphA2-derived T cell-epitopes promotes immunity against both EphA2-expressing and EphA2-negative tumors. J Transl Med. 2004;2(1):40. https://doi.org/10.1186/1479-5876-2-40.

22. Beauchamp A, Debinski W. Ephs and ephrins in cancer: ephrin-A1 signaling. Semin Cell Dev Biol. 2012;23(1):109–15.
23. Debinski W, Wykosky J. Molecular targeting of IL-13Rα2 and EphA2 receptor in GBM. Chapter 35. In: CNS cancer: models, prognostic factors and targets. Ed. Ervin van Meir, Springer, New York, NY, 2009. p. 841–858.
24. Hatano M, Eguchi J, Tatsumi T, Kuwashima N, Dusak JE, Kinch MS, et al. EphA2 as a glioma-associated antigen: a novel target for glioma vaccines. Neoplasia. 2005;7(8):717–22.
25. Binda E, Visioli A, Giani F, Lamorte G, Copetti M, Pitter KL, et al. The epha2 receptor drives self-renewal and tumorigenicity in stem-like tumor-propagating cells from human glioblastomas. Cancer Cell. 2012;22(6):765–580.
26. Miao H, Gale NW, Guo H, Qian J, Petty A, Kaspar J, et al. EphA2 promotes infiltrative invasion of glioma stem cells in vivo through cross-talk with Akt and regulates stem cell properties. Oncogene. 2014;34(5):558–67.
27. Debinski W. Drug cocktails for effective treatment of glioblastoma multiforme. Expert Rev Neurother. 2008;8(4):515–7.
28. Ferluga S, Tomé CM, Herpai DM, D'Agostino R, Debinski W. Simultaneous targeting of Eph receptors in glioblastoma. Oncotarget. 2016;7(37):59860–76.
29. Day BW, Stringer BW, Al-Ejeh F, Ting MJ, Wilson J, Ensbey KS, et al. EphA3 maintains tumorigenicity and is a therapeutic target in glioblastoma multiforme. Cancer Cell. 2013;23(2):238–48.
30. Nakada M, Niska JA, Miyamori H, McDonough WS, Wu J, Sato H, Berens ME. The phosphorylation of EphB2 receptor regulates migration and invasion of human glioma cells. Cancer Res. 2004;64(9):3179–85.
31. Liu W, Yu C, Li J, Fang J. The roles of EphB2 in cancer. Front Cell Dev Biol. 2022;10: 788587.
32. Rossmeisl JH, Herpai D, Quigley M, Cecere TE, Robertson JL, D'Agostino RB, et al. Phase I trial of convection-enhanced delivery of IL13RA2 and EPHA2 receptor targeted cytotoxins in dogs with spontaneous intracranial gliomas. Neuro Oncol. 2020;23(3):422–34.
33. Sharma P, Sonawane P, Herpai D, Rossmeisl J, Tatter S, Debinski W. Multireceptor targeting of glioblastoma. Neuro-Oncol Adv. 2020;2(1). https://doi.org/10.1093/noajnl/vdaa107.
34. Dai X, Cheng H, Bai Z, Li J. Breast cancer cell line classification and its relevance with breast tumor subtyping. J Cancer. 2017;8(16):3131–41.
35. Nakayama S, Torikoshi Y, Takahashi T. et al. Prediction of paclitaxel sensitivity by CDK1 and CDK2 activity in human breast cancer cells. Breast Cancer Res. 2009;11:R12.
36. Almeida-Ferreira C, Marto Carmo C, Almeida-Ferreira J, Frutuoso C, Carvalho MJ, Botelho MF, Laranjo M. Efficacy of cold atmospheric plasma vs. chemotherapy in triple-negative breast cancer: a systematic review. Int J Mol Sci. 2024;25: 3254.
37. Debinski W, Dickinson P, Rossmeisl JH, Robertson J, Gibo DM. New agents for targeting of IL-13RA2 expressed in primary human and canine brain tumors. PLoS ONE. 2013;8(10): e77719.
38. Barok M, Joensuu H, Isola J. Trastuzumab emtansine: mechanisms of action and drug resistance. Breast Cancer Res. 2014;16(2):209.
39. Prigent C, Dimitrov S. Phosphorylation of serine 10 in histone H3, what for? J Cell Sci. 2003;116(Pt 18):3677–85.
40. López-Otín C, Bond JS. Proteases: multifunctional enzymes in life and disease. J Biol Chem. 2008;283(45):30433–7.
41. Lopus M. Antibody-DM1 conjugates as cancer therapeutics. Cancer Lett. 2011;307(2):113–8.
42. Montemurro F, Delaloge S, Barrios CH, Wuerstlein R, Anton A, Brain E, et al. Trastuzumab emtansine (T-DM1) in patients with HER2-positive metastatic breast cancer and brain metastases: exploratory final analysis of cohort 1 from KAMILLA, a single-arm phase IIIb clinical trial. Ann Oncol. 2020;31(10):1350–8.
43. Mintz A, Gibo DM, Madhankumar AB, Debinski W. Molecular targeting with recombinant cytotoxins of interleukin-13 receptor alpha-2-expressing glioma. J Neuro-Oncol. 2003;64:117–23.
44. Sharma P, Roberts C, Herpai D, Fokt ID, Priebe W, Debinski W. Drug conjugates for targeting Eph receptors in glioblastoma. Pharmaceuticals (Basel). 2020;13(4): 77.
45. Kim C, Gao R, Sei E, Brandt R, Hartman J, Hatschek T, et al. Chemoresistance evolution in triple-negative breast cancer delineated by single-cell sequencing. Cell. 2018;173(4):879–93.
46. von Minckwitz G, Huang CS, Mano MS, Loibl, Mamounas EP, Untch M, Wolmark N, +22, for the KATHERINE Investigators. Trastuzumab emtansine for residual invasive HER2-positive breast cancer. N Engl J Med. 2019;380:617–628.
47. Simon S, Riddell SR. Dual targeting with CAR T cells to limit antigen escape in myeloma. Blood Cancer Discov. 2020;1(2):130–3.
48. Mishra A, Maiti R, Mohan, Gupta P. Antigen loss following CAR-T cell therapy: mechanisms, implications, and potential solutions. Eur J Haemat. 2024;112(2):211–222.

Publisher's Note

Waldemar Debinski has been Directing Brain Tumor Center of Excellence at Wake Forest University School of Medicine since 2004. He is an MD graduate of Warsaw Medical School in Poland and a PhD graduate of McGill University in Montreal, Canada, and did his postdoctoral training at the National Cancer Institute (NCI), Bethesda, MD as a Guest Researcher. The focus of his research has been molecular targeting for cancer treatment.